Chapter 17
Mesoscopic Modelling of Ultra-High Performance Fiber Reinforced Concrete Under Dynamic Loading

P. Forquin, J.L. Zinszner, and B. Lukic

Abstract For the two last decades numerous research works have been developed on the mechanical behavior of UHPFRC (Ultra-High Performance Fiber Reinforced Concrete) under quasi-static and dynamic loadings. However fibers orientation remains a major problem as during the implementation of fibers in concrete structure a random distribution and orientation of fibers is difficult to achieve. In this study four UHPFRC have been tested in dynamic tension and numerically simulated. The first concrete is made without any fibers. A random orientation of fibers is considered in the second concrete. Fibers oriented parallel or orthogonally to the loading direction (tensile loading) are considered in the two last cases. The four sets of concrete have been subjected to dynamic tensile loading by means of spalling tests. Next, a mesoscopic numerical simulation has been developed by considering a biphasic model: the concrete matrix is modelled by applying the DFH (Denoual-Forquin-Hild) anisotropic damage model to 3D finite-elements. In addition two nodes-finite elements are introduced in the 3D mesh to simulate numerically the presence of fibers by considering three orientations: fibers randomly distributed, parallel or orthogonal to the loading direction. As observed in the experiments, a small influence of fibers is observed regarding the peak-stress whereas a strong influence of fibers orientation is noted regarding the post-peak tensile response of UHPFRC.

Keywords Concrete • Spalling tests • Damage • Fibers • mesoscopic modeling

17.1 Introduction

For several years, the dynamic behavior of Ultra-High Performance Concretes (UHPC) is investigated due to their exquisite material properties. The quasi-static compressive strength of concretes has increased considerably over the last 20 years [1]. In the middle of the 1990s, the use of superplastifiers, silica fumes and quartz grains led to production of UHPC concrete materials with a compressive strength of about 200 MPa [2], that were outstanding compared with that of ordinary concrete. Research programs that aim at evaluating ballistic performance of ultra-high strength concrete are currently under way. One of the goals is to improve the understanding and modeling of damage mechanisms under impact [3]. In the present study, a UHPC similar to that of Ductal® concrete produced by Lafarge is investigated under different loading conditions. Besides its compressive strength (200 MPa), this UHPC is of interest to be produced on an industrial scale. Significant increase of flexural strength and ductility is obtained by adding fibers during the mixing process [4]. However, the potential effects of fiber content under extreme loading conditions such as impact of rigid projectile needs to be thoroughly investigated. The present work aims at evaluating the influence of fibers under three different types of loadings: dynamic tensile loading, confined compression loading and dynamic shear loading.

Indeed, during the impact of a rigid projectile against a concrete target severe damage modes are observed such as spalling on the front face, radial cracking in the whole target and, in case of the perforation, scabbing on the rear face [5]. Moreover, high confining pressures are observed in front of the projectile involving mechanisms such as micro-cracking and collapse of porosity [6]. Both confined and tensile behaviors are influencing the penetration resistance of the target [7]. Therefore, the constitutive model used in numerical simulations of a penetrating rigid projectile in a concrete target, should take into account the concrete confined behavior and the tensile resistance of concrete at high strain rates.

In the present work, dynamic tensile tests (spalling tests) are performed with a Hopkinson Pressure Bar. Furthermore, the tensile behavior of UHPC is investigated through mesoscopic modeling. Finally, the numerical predictions are compared to experimental data to assess the predictive capabilities of the mesoscopic model.

P. Forquin (✉) • J.L. Zinszner • B. Lukic
Soils Solids Structures Risks (3SR) Laboratory, Grenoble-Alps University, 38041, Grenoble Cedex 9, France
e-mail: pascal.forquin@3sr-grenoble.fr

D. Casem et al. (eds.), *Dynamic Behavior of Materials, Volume 1*, Conference Proceedings
of the Society for Experimental Mechanics Series, DOI 10.1007/978-3-319-41132-3_17

Table 17.1 Material composition and mechanical properties of an Ultra-High Performance Concrete [3]

Composition		UHPC
Cement	[kg/m^3]	*730*
Silica fume	[kg/m^3]	*235*
Crushed quartz grains	[kg/m^3]	*220*
Sand	[kg/m^3]	*885*
Superplasticizer	[kg/m^3]	*10*
Water	[l/m^3]	*160*
Steel fibers	[vol. %]	*2 %*
W/(C + SF)		*0.17*
Mechanical Properties		
Density	[kg/m^3]	*2396*
Young's modulus	[GPa]	55
Quasi-static compressive strength	[MPa]	200

17.2 Tested Concrete

17.2.1 Composition of UHPC

The material investigated is an Ultra High Performance Concrete (UHPC) whose mechanical properties and composition are gathered in Table 17.1. In contrast to conventional concrete, apart from cement, sand and water, it contains finely crushed quartz grains and silica fume. The optimized granular mixture of UHPC, where the maximal grain size is approximately 0.6 mm (sand), and extremely low water to cementious material (cement and silica fumes) ratio allows casting a concrete with outstanding mechanical properties. The use of superplasticizer in order to increase the workability is of great importance. In the present work, four sets of specimens have been considered for dynamic spalling testing: one which contains 2 % volumetric ratio of short steel fibers (0.2 mm diameter and 7 mm in length) with 3 types of orientation (random orientation, well or badly oriented fibers) and the other without additional fiber reinforcement.

17.2.2 Mixing and Casting of UHPC and Concrete Samples

The specimens used in spalling testing are cylinders of diameter around 46 and 140 mm in length. The specimens were cored out from large blocks ($270 \times 270 \times 170\,\text{mm}^3$) more than 40 days after the mix was poured into watertight plywood moulds. All the samples had been stored in water saturated by lime in order to avoid the dissolution of portlandite into water.

17.3 Experimental Results

The device used to perform the Spalling experiments is described on the Fig. 17.1. The gas gun, of caliber 50 mm, is used to launch small cylindrical projectile at impact velocity ranging from 1 to 20 m/s. The spalling test set-up used in this study is composed of a 50 mm-long spherical-cap-ended projectile and a Hopkinson bar both with a diameter of 45 mm. An illustration of the experimental set-up is given on Fig. 17.1. A short incident compressive pulse is created and propagates through the Hopkinson bar. Then, the pulse is transmitted to the sample and reflects at the free-end of the specimen as a tensile pulse leading to a dynamic tensile loading within the sample. The particle velocity at the rear-face is recorded with a laser interferometer, enabling velocity measurements up to 20 m/s with 1.5 MHz bandwidth [8].

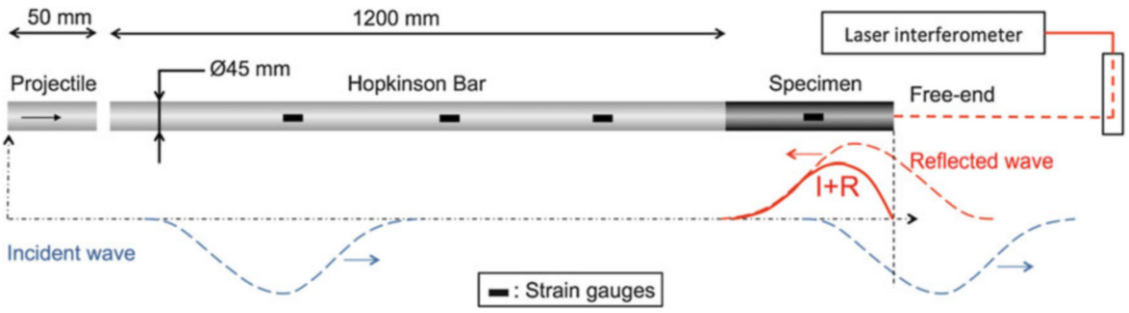

Fig. 17.1 Experimental device for spalling tests

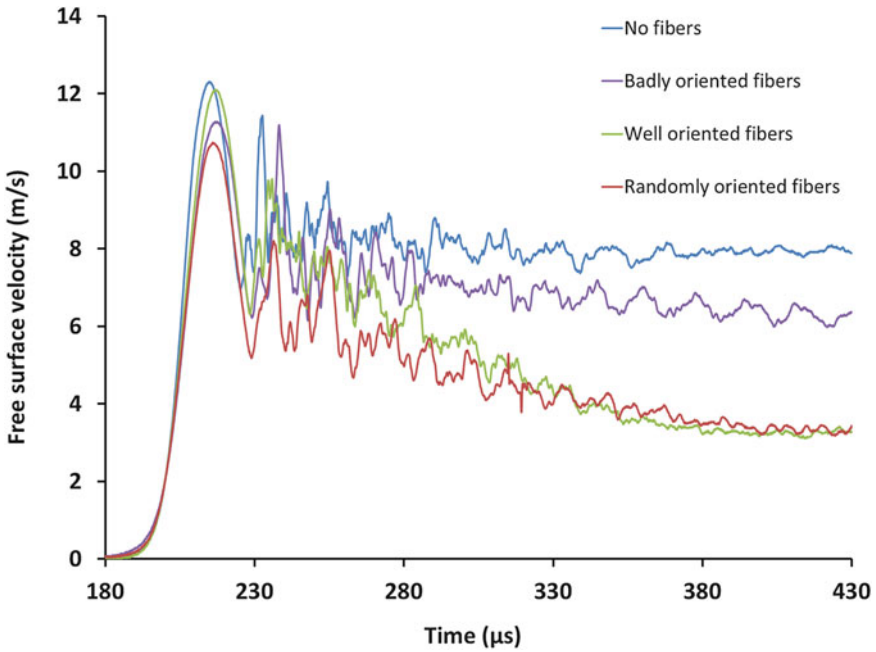

Fig. 17.2 Particle velocity profiles recorded on the rear free surface of samples subjected to spalling test

The particle velocity profile recorded on the rear free surface of four different samples is plotted on the Fig. 17.2. Based on the Novikov et al. [9] approach, one can estimate the dynamic tensile strength of the each sample from the pullback velocity (the difference between the maximum speed and the speed corresponding to rebound) assuming a linear elastic behavior of the material before to reaching the tensile ultimate strength:

$$\sigma_{dyn} = \frac{1}{2}\rho C_0 \Delta V_{pb} \tag{17.1}$$

where ρ is the density, C_0 is the one dimensional wave velocity (about 4790 m/s) in the material and ΔV_{pb} is the pullback velocity. A dynamic tensile strength of 30 MPa is obtained whatever the tested sample.

17.4 DFH Anisotropic Damage Model

In the present work, the Denoual-Forquin-Hild modeling [10, 11] is employed to model the tensile behavior of UHPC without fibers. Under high strain rate conditions, several cracks are initiated and propagate from the initial defects leading to multiple fragmentation. In that case, while the weakest defect is activated and propagates, several other cracks

are initiated during this time. As the loading rate is high, there is enough time for the stress level to reach high levels and activate smaller defects. The multiple fragmentation process with multiple cracks growing at the same time stops when the whole structure is covered by these relaxed stress regions. The interaction law between cracks already initiated and the critical defects of the material is given by the concept of probability of non-obscuration P_{no} [10, 11]. In the case of multiple fragmentations, the interaction between the horizon (the region around a crack where stresses are relaxed due to crack opening) and the boundary of the domain Ω is small and if a uniform stress field is assumed, the obscuration probability P_o is written as [11]

$$P_o(T) = 1 - P_{no}(T) = 1 - \exp\left(-\int_0^T \frac{d\lambda_t}{dt}[\sigma(t)]\ Z_o(T-t)dt \right) \tag{17.2}$$

In Eq. 17.2, Z_o is the obscured zone, σ the local principal stress component, T the current time and t the crack initiation time. The probability of obscuration is defined for each eigen direction i and the change of P_i is expressed in differential form, in order to be employed in an FE code using Eq. 17.3, as

$$\frac{d^2}{dt^2}\left(\frac{1}{1-P_i}\frac{dP_i}{dt}\right) = 3!S(kC_0)^3\lambda_t[\sigma_i(t)] \ \text{ when } \ \frac{d\sigma_i}{dt} > 0 \ \text{ and } \ \sigma_i > 0 \tag{17.3}$$

where σ_i is the local principal stress component. The macroscopic strength of the material is described as the microscopic stress in the non-obscured zones and a cohesive stress in the obscured zones that controls the softening behavior of the material [12].

$$\Sigma_i = (1 - P_{oi})\sigma_i + (P_{oi})^{\alpha_D}\sigma_{coh}(\varepsilon) = (1 - D_i)\sigma_i, \tag{17.4}$$

where D_i is the damage variable defined for each principal direction and σ_{coh} is the residual strength in the obscuration zone:

$$\sigma_{coh} = \sigma_o^d \exp\left(-\left(\frac{\varepsilon}{\varepsilon_0^d}\right)^{n_d} \right) \tag{17.5}$$

where α_D, σ_o^d, ε_o^d, n_d are material-dependent parameters that were identified for the non-fibered concrete.

17.5 Numerical Simulations

A series of numerical simulation were conducted with Abaqus Explicit Finite-Element code. The concrete sample is meshed with C3D8R elements and 2-nodes T3D2 elements are used for the fibers. The fibers are embedded in the concrete mesh. An elasto-plastic behavior (yield strength: 1800 MPa) is assumed for the fibers whereas the DFH model is used to model the concrete matrix. The experimental compressive pulse is applied to the "contact" sample end. Finally, the particle velocity measured on the rear free-end is compared to experimental data on the next figures considering randomly oriented fibers (Fig. 17.3), badly oriented fibers (Fig. 17.4) and well oriented fibers (Fig. 17.5).

Finally, the mesoscopic calculations enable to predict the rebound of particle velocity that corresponds to the peak strength of the concrete. In addition, the continuous decrease of particle velocity noted in the cases of randomly-oriented and well-oriented fibers is well captured by the mesoscopic modeling whereas particle velocity plateau noted in the case of badly oriented fibers is well predicted.

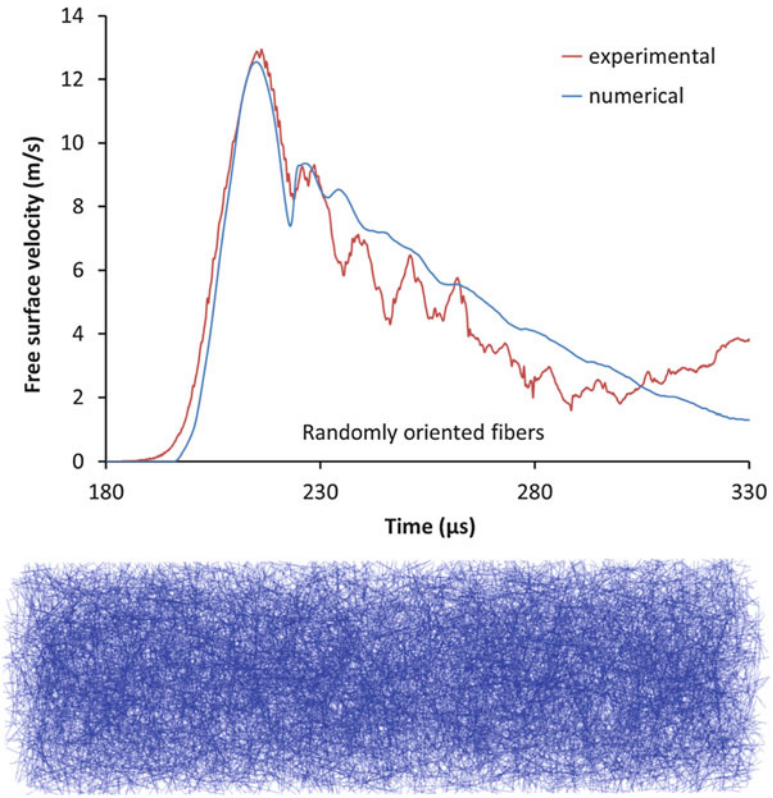

Fig. 17.3 Spalling test performed with randomly oriented fibers. Comparison of experimental and numerical data

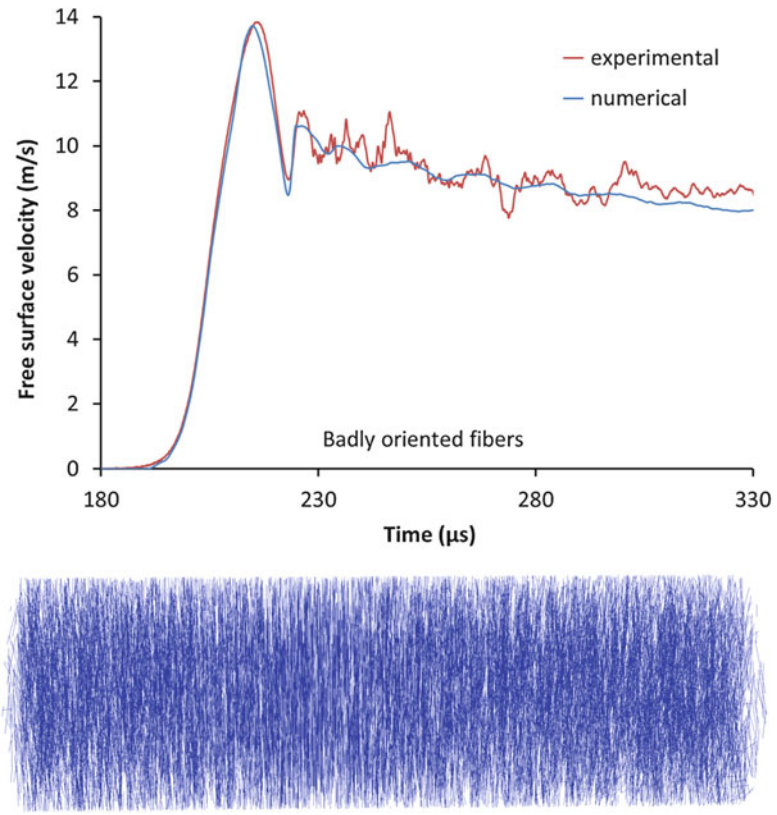

Fig. 17.4 Spalling test performed with badly oriented fibers. Comparison of experimental and numerical data

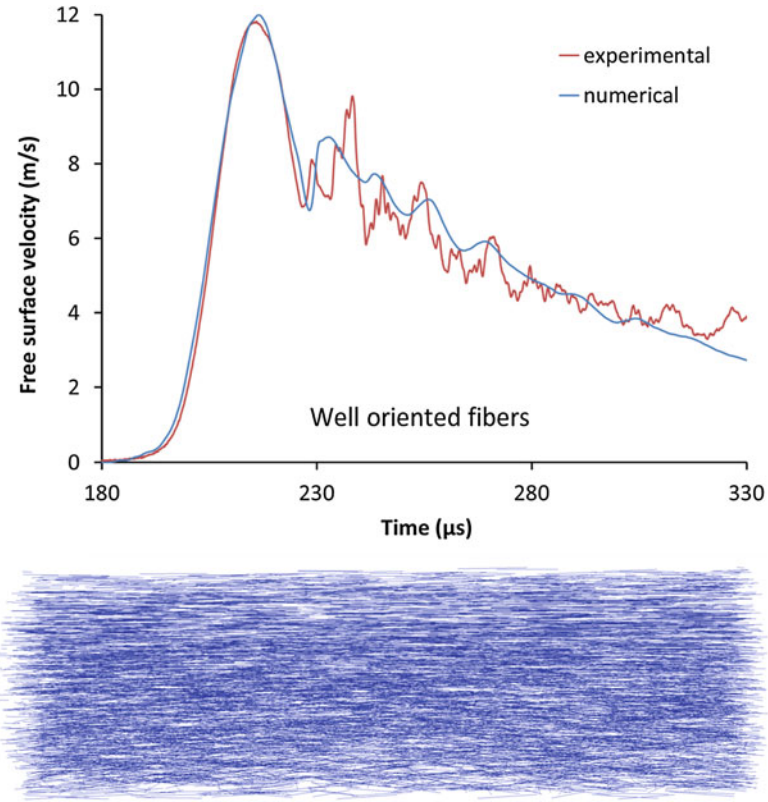

Fig. 17.5 Spalling test performed with well oriented fibers. Comparison of experimental and numerical data

17.6 Conclusion

In conclusion, the dynamic tensile behavior of an UHPC (Ultra-High Performance Concrete) with and without steel fiber reinforcement has been investigated through spalling tests. A Hopkinson Pressure Bar (HPB) device is used and a laser interferometer is pointed out toward the rear free-end of the samples allows deducing the particle velocity. Whereas the peak stress obtained through the Novikov formula is weakly influenced by fibers and fibers orientation, a clear influence of fibers is noted regarding the tail of velocity profiles. In addition, a mesoscopic modeling was used to simulate numerically the experiments by differentiating the behavior of the concrete matrix (use of DFH Denoual-Forquin-Hild anisotropic damage model) and the behavior of the fibers (elasto-plastic model). Finally the mesoscopic calculations are able to reproduce the peak strength and the post-peak responses of the fibered concretes whatever the orientation of fibers.

Aknowledgment This work was supported by the CEA (French Alternative Energies and Atomic Energy Commission, Centre de Gramat). This support is gratefully acknowledged.

References

1. Malier Y.: Les bétons à hautes performances, l'Ecole Nationale des Ponts et Chaussées, France, 1992
2. Richard P., Cheyrezy M.: Composition of reactive powder concretes, vol. 25, no. 7, pp. 1501–1511, 1995
3. Forquin, P., Hild, F.: Dynamic fragmentation of an ultra-high strength concrete during edge-on impact tests. J. Eng. Mech. **4**(134), 302–315 (2008)
4. Bayard O.: Approche multi-échelles du comportement mécanique des bétons à ultra hautes performances renforcés par des fibres courtes, Ecole Normale Supérieure de Cachan, 2003
5. Li, Q.M., Reid, S.R., Wen, H.M., Telford, A.R.: Local impact effects of hard missiles on concrete targets. Int. J. Impact Eng. **32**(1–4), 224–284 (2005)
6. Forquin, P., Arias, A., Zaera, R.: Role of porosity in controlling the mechanical and impact behaviours of cement-based materials. Int. J. Impact Eng. **35**(3), 133–146 (2008)
7. Forquin, P., Sallier, L., Pontiroli, C.: A numerical study on the influence of free water content on the ballistic performances of plain concrete targets. Mech. Mater. **89**, 176–189 (2015)

8. Erzar, B., Forquin, P.: An experimental method to determine the tensile strength of concrete at high rates of strain. Exp. Mech. **50**(7), 941–955 (2010)
9. Novikov, S.A., Divnov, I.I., Ivanov, A.G.: The study of fracture of steel, aluminium and copper under explosive loading. Fiz. Met. Metalloved **21**, 608–615 (1966)
10. Denoual, C., Hild, F.: A damage model for the dynamic fragmentation of brittle solids. Comput. Methods Appl. Mech. Eng. **183**(3), 247–258 (2000)
11. Forquin, P., Hild, F.: A probabilistic damage model of the dynamic fragmentation process in brittle materials. Adv. Appl. Mech. **44**, 1–72 (2010)
12. Erzar, B., Forquin, P.: Analysis and modelling of the cohesion strength of concrete at high strain-rates. Int. J. Solids Struct. **51**(14), 2559–2574 (2014)